J. Membrane Biol. 178, 89–101 (2000)
DOI: 10.1007/s002320010017

The Journal of
Membrane
Biology

Isoform-Specific Function and Distribution of Na/K Pumps in the Frog Lens Epithelium

J. Gao[1], X. Sun[1], V. Yatsula[1], R.S. Wymore[2], R.T. Mathias[1]
[1]Department of Physiology & Biophysics, SUNY at Stony Brook, NY 11794-8661, USA
[2]Department of Biological Science, University of Tulsa, Tulsa, OK 74104-3189, USA

Received: 17 May 2000/Revised: 11 August 2000

Abstract. Epithelial cells from the anterior and equatorial surfaces of the frog lens were isolated and used the same day for studies of the Na/K ATPase. RNase protection assays showed that all cells express α_1- and α_2-isoforms of the Na/K pump but not the α_3-isoform, however the α_2-isoform dominates in anterior cells whereas the α_1-isoform dominates in equatorial cells. The whole cell patch-clamp technique was used to record functional properties of the Na/K pump current (I_P), defined as the current specifically inhibited by dihydro-ouabain (DHO). DHO-I_P blockade data indicate the α_1-isoform has a dissociation constant of 100 μM DHO whereas for the α_2-isoform it is 0.75 μM DHO. Both α_1- and α_2-isoforms are half maximally activated at an intracellular Na^+-concentration of 9 mM. The α_1-isoform is half maximally activated at an extracellular K^+-concentration of 3.9 mM whereas for the α_2-isoform, half maximal activation occurs at 0.4 mM. Lastly, transport by the α_1-isoform is inhibited by a drop in extracellular pH, which does not affect transport by the α_2-isoform. Under normal physiological conditions, I_P in equatorial cells is approximately 0.23 μA/μF, and in anterior cells it is about 0.14 μA/μF. These current densities refer to the area of cell membrane assuming a capacitance of around 1 μF/cm^2. Because cell size and geometry are different at the equatorial *vs.* anterior surface of the intact lens, we estimate Na/K pump current density per area of lens surface to be around 10 μA/cm^2 at the equator *vs.* 0.5 μA/cm^2 at the anterior pole.

Key words: Na/K ATPase — Lens — α-Isoforms — Whole cell patch clamp — Na^+-dependence — K^+-dependence — pH

Correspondence to: R. Mathias

Introduction

The lens and cornea work in series to focus light on the retina. Because they are directly in the optical path to the retina, neither tissue has blood vessels, which would scatter light. The lack of blood supply poses some special problems for homeostasis in the lens. A recent review (Mathias, Rae & Baldo, 1997) summarizes much of what is known about the properties and localization of transport proteins in the lens, and how these relate to homeostasis. The conclusions expressed in that review are summarized below.

The lens has no blood borne delivery of O_2 and glucose or removal of CO_2 and wastes, and in most animals the lens is too large for diffusion to effectively support the needs of the interior fiber cells. To compensate, interior fiber cells have a very low rate of metabolism that is entirely anaerobic. Nevertheless, the metabolic rate is not zero and it still requires the delivery of glucose and removal of waists. Moreover, interior fiber cells need to maintain low Ca^{2+}-, low Na^+-, high K^+-concentration and normal pH, yet they cannot afford to expend metabolic energy regulating these ions. To minimize the leak of ions, fiber cells have very high resistance membranes. An extensive network of gap junctions connects interior fibers to surface cells, where metabolic energy can be used to transport Na^+, Ca^{2+} and H^+ out of the lens cells and K^+ into lens cells. Despite the high resistance of fiber cell membrane, there will be a small leak of Na^+, from its high concentration in the extracellular space between fibers, down its electrochemical gradient into each fiber cell. There are far more interior fiber cells than surface cells that provide the active transport, so even though the leak of Na^+ into each fiber cell is small, in total it becomes significant. Mathias (1985) (reviewed in Mathias and Rae, 1985) proposed a standing, circulating Na^+-current flowed between the interior fiber cells and surface cells, and hy-

pothesized that this flux of solute creates a circulation of fluid that is an internal circulatory system for the avascular lens.

The model envisioned by Mathias (1985) had Na^+ flowing uniformly into the lens along the extracellular spaces, crossing a fiber cell membrane, then flowing from cell to cell via gap junctions to the surface, where the Na/K pumps were assumed to be uniformly distributed. Robinson and Patterson (1983) published the first of a series of papers in which they showed the lens did indeed have an internal circulating current, however it was not uniform. Instead, it enters the lens at both poles and exits at the equator (*see* Fig. 1). Baldo and Mathias (1992) looked for spatial variations in the passive electrical properties of the lens that might be connected with this circulating current. They found gap junctional coupling in the outer shell of differentiating fiber cells (DF in Fig. 1) was primarily concentrated at the equator. Mathias et al. (1997) modified the model of circulating Na^+ to have the cell-to-cell current be directed to the equatorial surface by the low resistance equatorial gap junctions. The model still assumed the water permeability of lens cell membranes was sufficiently high for fluid to follow the circulation of Na^+, but now the internal circulatory system was more efficiently designed to create a well stirred intracellular compartment.

There were two weaknesses in the model calculations of Mathias et al. (1997). First, the value of membrane water permeability was not known, so it was assumed to be sufficiently high that fluid followed solute transport essentially isotonically. Varadaraj et al. (1999) measured fiber and epithelial cell membrane water permeabilities and found each was indeed sufficiently high that this assumption was valid. Second, the pole to equator distribution of Na/K pump current in surface cells was not known, so it was assumed to be uniform. The intracellular current flow through gap junctions to the equatorial surface was calculated based on the electrochemical gradient for Na^+ to enter fiber cells, the measured Na^+-conductance of fiber cell membrane, and the measured distribution of gap junctional conductance. The predicted current flow into an equatorial surface cell via gap junctions was about the same as the current measured by Robinson and Patterson (1983) just outside of equatorial cells. The model assumed that whatever gap junctional current flowed into a surface equatorial cell would exit across that cell's membrane. The mechanism was assumed to be depolarization of the transmembrane voltage in equatorial cells. The purpose of the present study was to measure the transport of Na/K by anterior epithelial cells and equatorial epithelial/differentiating cells (red cells in Fig. 1). In particular, we were interested in the properties and distribution of the Na/K pumps.

Materials and Methods

Cell Isolation

Frogs (*Rana pipiens*) were sacrificed by pithing; their eyes were then removed, placed in Ca^{2+} free Ringer solution and the lens carefully dissected free. The cell isolation procedure followed that described in Cooper, Rae & Gates (1989). The capsule was mechanically peeled from the posterior of the lens, partially cut to form four flaps and pinned in sylgard. A circle, centered on the anterior pole with a radius of approximately half the distance from pole to equator was cut out. This circle of anterior epithelial cells was separated from the remaining equatorial cells. The anterior and equatorial pieces of capsule with their adhering cells were placed in Ringer solution containing 0.05% trypsin (Sigma type III) and 30 μM Ca^{2+}. After 20 min, the pieces of capsule with adhering cells were returned to Ca^{2+}-free Ringer, where they were torn into smaller pieces using forceps. These pieces were gently triturated, causing many cells to break free and be available for whole cell patch-clamp studies. The equatorial cells could be further classified as either epithelial (cuboidal) or differentiating (elongated).

Solutions

Ca^{2+}-free Ringer solution contained (in mM): NaCl 102.5, NaOH 2, KCl 2.5, $MgCl_2$ 1.5, Hepes 5, Glucose 5, pH = 7.35. The perfusion solution contained (in mM): NaCl 102.5, NaOH 2, KCl 8, $MgCl_2$ 1.5, HEPES 5, Glucose 5, $BaCl_2$ 0.5, $CdCl_2$ 0.2, pH = 7.35. The pipette solution contained (in mM): K-Aspartic Acid 50, Na-Aspartic Acid 40, KOH 2, $MgCl_2$ 3, HEPES 5, glucose 5, Na_2ATP 5, pH = 7.1. These solutions were designed to minimize currents carried by ion channels and thus maximize signal to noise when measuring Na/K pump current (I_P). Ba^{2+} and Cd^{2+} were used to reduce K^+- and Ca^{2+}-conductances. High external K^+ and internal Na^+ concentrations were used to increase I_P and thus improve the signal-to-noise ratio. In experiments which used varied $[Na^+]_i$, Na^+-Aspartic Acid was exchanged for K^+-Aspartic Acid. In experiments that varied $[K^+]_o$, NaCl was substituted for KCl. To reduce the pH of the external solution, HCl was added.

Cloning Na/K Pump α-Subunit Probes

Degenerate oligonucleotide primers for the α-subunit of the Na/K pump (Gao et al., 1999) were used to screen *Rana pipien*s brain by PCR for the 3 α-isoforms.

Upstream	K	N	C	L	V	K	N
Primer	5′-aa(a/g)	aa(c/t)	tg(c/t)	(c/t)t(a/c/g/t)	gt(c/g)	aa(a/g)	aa(c/t)-3′
Downstream	5′-(c/t)tt	(a/g)tt	(g/t)gt	(a/c/g/t)(c/g)(a/t)	(a/g)tt	(a/g)aa	(g/c)gg-3′
Primer	K	N	T	S	N	F	P

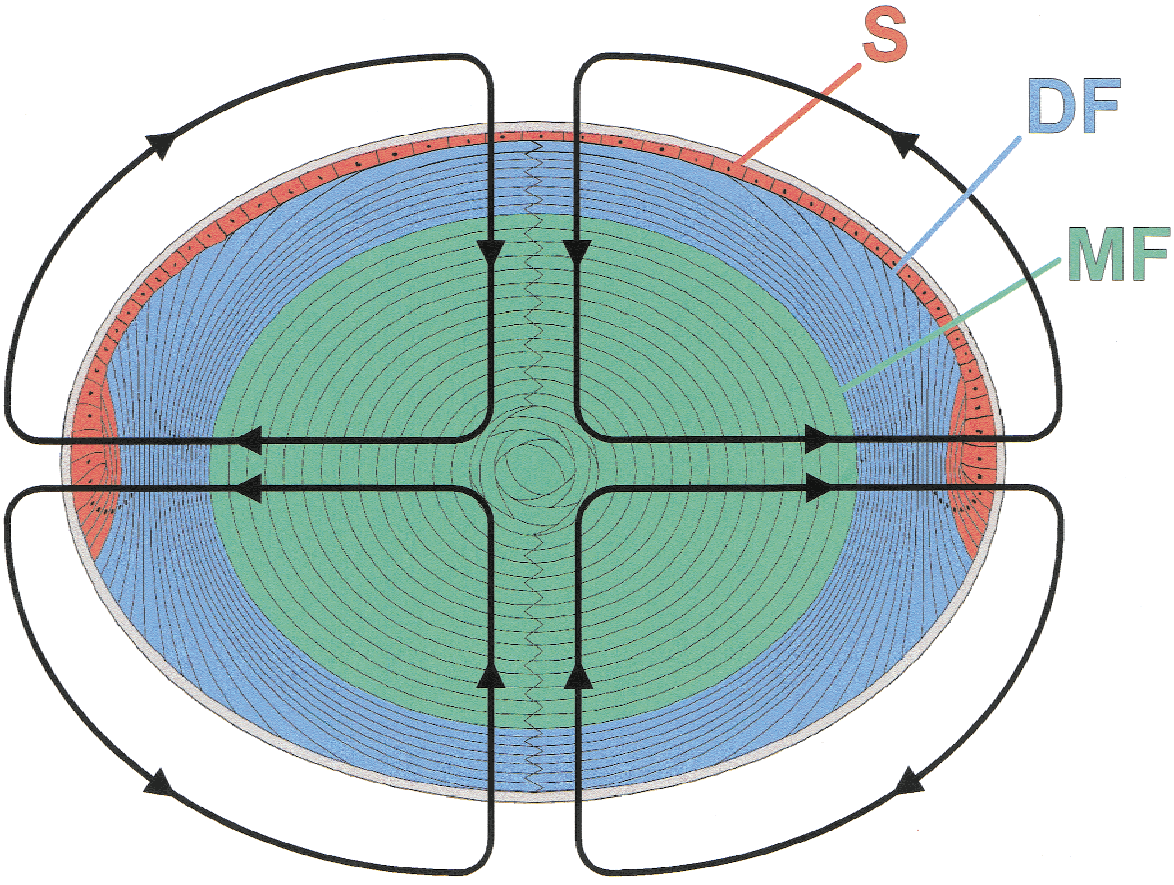

Fig. 1. The cellular structure of the lens with the lines of circulating current flow superimposed. Three cell types can be functionally distinguished. About 50% of the volume of a small frog lens is composed of the central mature fibers (MF shown in green), which have no organelles or active membrane transport, but are connected to the surface by gap junctions. A significant part of the leak of Na^+ into lens cells is thought to occur across these membranes. Next is an outer shell of differentiating fibers (DF shown in blue) that are in the process of losing organelles and may have limited active membrane transport at their basal ends, which are in contact with the posterior capsule. Although this layer extends only about 20% of the distance into the lens, it contains nearly 50% of the total membrane area and thus represents another significant path for the leak of Na^+ into lens cells. The outer single layer of surface cells (S shown in red) is the anterior epithelium, whose cells at the equator begin to elongate and are referred to in the text as differentiating cells. This layer represents less than 2% of the total membrane area yet it is responsible for nearly all of the active transport of Na^+ out of lens cells via the Na/K ATPase. The cells shown in red were acutely isolated and used for whole cell patch clamp studies of the lens Na/K pumps.

Bam H1 and EcoR1 cloning sites were added to the 5′ and 3′ ends of the primers respectively. Brain poly A^+ RNA was reverse transcribed using Super Script II reverse transcriptase (Gibco BRL). The above two primers and brain cDNA were used for PCR. A product of about 400 bp was cloned in pBluescript SK^+ (Stratagene) and sequenced (sequenase vertion 2, USB). The subunits were identified by comparing them to published sequences using NIH Gene Bank BLAST search.

RNase Protection Assays

Poly A^+ RNA was isolated using paramagnetic poly dt beads (Dynal). All other steps were performed according to the protocol supplied with the kit. For brain poly A^+ RNA extraction, approximately 50 mg of tissue was used. About 50 lenses were required to obtain less than 1 mg tissue for anterior epithelial cell and equatorial epithelial/differentiating cell poly A^+ RNA extractions.

Preparation of antisense RNA probes and the RNase protection assays were performed as described in Kreig and Melton (1987) and Wymore et al. (1997). A frog cyclophilin probe was PCR cloned using available sequence data to design primers. The cyclophilin was included in the hybridization reaction to confirm that the sample was not lost and also to provide a standard band in each gel to which the bands for different Na/K pump α-isoforms could be compared. Yeast tRNA (5 μg) was used as a negative control for probe self-protection bands. The RNA was divided equally for each sample (less than 0.1 μg poly A^+ RNA per sample). To determine the amounts of α_1-, α_2-, and α_3-isoform mRNA, the gels were exposed overnight and the intensity of specific bands measured using a Phosphor Imager (Storm 860, Molecular Dynamics).

Whole Cell Patch Clamp

The isolated cells were placed in a chamber in which the perfusion solution could be exchanged with a time constant of 13 sec. A glass

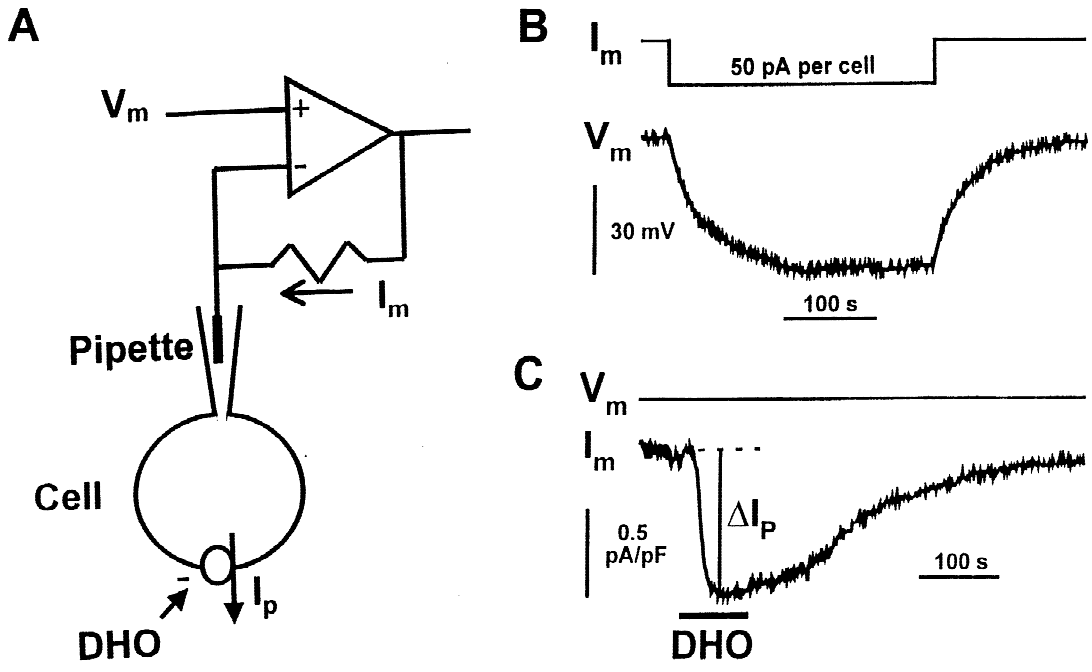

Fig. 2. The whole cell patch-clamp method of measuring total cell capacitance and Na/K pump current. (*A*) The whole cell patch configuration. (*B*) The current-clamp configuration allows injection of a pulse of membrane current (I_m) while recording the time course of the change in membrane voltage (V_m). $V_m(t)$ is curve fit with Eq. 1 to obtain total cell capacitance (C_m). (*C*) The voltage-clamp configuration of the whole cell patch clamp allows V_m to be held constant while recording the time course of the change in I_m following a brief superfusion of the cell with Ringer solution containing dihydro-oubain (DHO). The steady-state shift in inward current is directly proportional to the fraction (ΔI_P) of outward Na/K pump current (I_P) blocked by the concentration of DHO superfused.

patch pipette (initial resistance of about 5 MΩ) was gently pressed against the cell and suction applied until the pipette sealed to the membrane (seal resistance of 10–20 GΩ). Further suction caused the patch of membrane beneath the tip to rupture (*see* Fig. 2*A*) and within about 1 min the pipette solution had exchanged with the cell's contents and the holding current stabilized. To measure membrane capacitance, C_m (*F*), and conductance, G_m (*S*), and pipette resistance, R_P (Ω), the Axopatch 1B amplifier (Axon Instruments, Foster City, CA) was switched to current clamp mode and a square pulse of current was injected into the cell (*see* Fig 2*B*). The time course of the response $V_m(t)/I_m$ is given by

$$\frac{V_m(t)}{I_m} = R_p + \frac{1}{G_m}(1 - e^{-tG_m/C_m}) \tag{1}$$

Data such as those shown in Fig. 2*B* were curve fit with Eq. 1 to determine C_m and G_m. To measure Na/K pump current (I_P), a stock solution containing 85 mM dihydro-ouabain (DHO), a specific inhibitor of the Na/K pump, was added to the perfusion solution to achieve the desired concentration of DHO. While the cell was voltage clamped at 0 mV, the change in membrane current (ΔI_P) in Fig. 2*C* due to superfusion of DHO was recorded and assumed to represent blockade of some fraction of I_P. A saturating concentration of DHO therefore provides a measure of total Na/K ATPase activity.

All of the data reported here were obtained through population studies of many different cells. This was necessary because the whole cell patch clamp of lens cells could not be routinely maintained for a sufficiently long period to record I_P in the same cell in more than one environment. Thus, for example, to determine the effect on I_P of changing $[K^+]_o$ from 1 to 8 mM, we recorded from about 10 different cells at each $[K^+]_o$. To control for cell-to-cell variability in size, the capacitance of each cell was measured as an estimate of membrane area, then the pump current was normalized by the input capacitance. There is also, however, cell-to-cell variability in the density of Na/K pump protein and in the fraction of each isoform expressed, and these factors are not controlled in a population study. In contrast, for the larger, more robust mammalian heart cells, we measured isoform-specific I_P at two values of $[K^+]_o$ in the same cell, then normalized the value of I_P at each test $[K^+]_o$ to the value recorded in 8 mM $[K^+]_o$ (Gao et al., 1995). This procedure controls for variability in isoform expression, pump density and cell size, hence the data are intrinsically more accurate. Because of this limitation in the study of lens cells, the studies reported here are not as extensive as those in Gao et al. (1995) and we specifically looked for effects similar to those measured in the mammalian heart cells.

Theoretical Model of I_P

Based on the data which follow, each lens epithelial/differentiating cell expresses the α_1- and α_2-isoform of the Na/K pump, hence total pump current, I_P, is the sum of the current generated by the α_1- and α_2-isoforms:

$$I_P = I_{P1} + I_{P2}. \tag{2}$$

In the presence of DHO, each isoform is inhibited with different dissociation constants, so I_P-blockade by DHO is described by:

$$I_p = I_{P1}\frac{K_{D1}}{[DHO] + K_{D1}} + I_{p2}\frac{K_{D2}}{[DHO] + K_{D2}} \tag{3}$$

Although the relative contributions of I_{P1} and I_{P2} vary dramatically from anterior pole to equator, the dependencies of I_{P1} and I_{P2} on $[Na^+]_i$, $[K^+]_o$ and pH_o are assumed to be intrinsic properties of each isoform. Based on work described in Gao et al. (1995) in mammalian heart cells, the effects of the ionic environment on either isoform can be described by:

$$I_{p1} = I_{max1}\left(\frac{[Na^+]_i}{[Na^+]_i + K_{Na1}}\right)^3\left(\frac{[K^+]_o}{[K^+]_o + K_{K1}}\right)^2\left(\frac{K_H}{K_H + [H^+]_o}\right)$$

$$I_{p2} = I_{max2}\left(\frac{[Na^+]_i}{[Na^+]_i + K_{Na2}}\right)^3\left(\frac{[K^+]_o}{[K^+]_o + K_{K2}}\right)^2 \quad (4)$$

Equation 4 models the effects of Na^+ and K^+ as being independent, whereas for a cyclic enzyme like the Na/K ATPase, one would expect them to be interdependent. Nevertheless, Gao et al. (1995) found that, in physiological conditions, the effects were approximately independent and adequately modeled by Eq. 4. Moreover, in this model (Eq. 4), $[Na^+]_i$ binds to 3 independent, identical sites. Similarly, $[K^+]_o$ binds to 2 independent, identical sites. These idealized models adequately fit the experimental data, but should not be considered accurate reflections of molecular events. Lastly, our data suggest H^+ binds to an external site on the α_1-isoform and causes inhibition of transport. The α_2-isoform appears to lack this H^+-binding site. Equations 2–4 were used to analyze our data.

In the Results, I_{max1} and I_{max2} are assumed to be proportional to the amounts of α_1- and α_2-protein, respectively, with the ATPase activity per protein being approximately equal. Thus the fraction of α_1-isoform protein present in a cell would be given by $I_{max1}/(I_{max1} + I_{max2})$. However, because I_{P1} and I_{P2} have different dependencies on the ionic environment, particularly on $[K^+]_o$ and $[H^+]_o$, the fraction of I_{P1} is given by $I_{P1}/(I_{P1} + I_{P2})$, which is not the same as the fraction of protein. Indeed, the fraction of current will vary depending on the environment. Thus, to analyze our data, we assume the amount of protein is proportional to the amount of mRNA and base I_{max1} and I_{max2} on the RNase protection results, then the fractions of I_{P1} and I_{P2} are estimated using Eqs. 2 and 4 with experimentally determined dissociation constants.

Results

There have been reports that in different regions, mammalian lens epithelial cells express different α-isoforms of the Na/K pump (Garner & Horwitz, 1994; Garner, 1994; Mosley, Dean & Delamere, 1996; Tao, Hollenberg & Graves, 1999; Garner & Kong, 1999). Moreover, our data on DHO-blockade of I_P in frog lens epithelial cells suggested the anterior and equatorial cells express different α-isoforms, since the affinity of anterior cells for DHO was much higher than that of equatorial cells (*see* the next section). We therefore performed RNase protection assays to determine which α-isoforms were expressed in these two domains.

RNase Protection Assays

Figure 3*A* shows the alignment of amino acid sequences for the fragments of the different α-isoforms cloned from frog brain. The blanks indicate identical amino acids whereas the differences are listed. The α_1-, α_2-, and α_3-isoforms were identified based on comparison of these fragments with published sequences (Fig. 3*B*). Figure 3*C* shows the results of the RNase protection assays. The first lane (probes) in each gel shows undigested antisense cRNA probes. The second lane (tRNA) is empty, indicating there is no self protection of the probe. The last lane (brain) shows success of the RNase protection assay in brain, where we know all 3 isoforms of the Na/K pumps and cyclophilin (cyc) are present. The gel on the right hand side indicates there is no α_3-isoform present in epithelial cells from the anterior or equator of frog lenses. The cyc-band in this photograph is not visible but could be faintly seen in the original film whereas the α_3-band could not be detected. The bands for the α_1- and α_2-isoforms were much stronger than that for cyc, so relatively little, if any, α_3-isoform mRNA is present. The left hand and central gels indicate both the α_1- and α_2-isoforms are present in anterior and equatorial cells, however the fraction of α_1 is quite different in these two domains. We used the ratio of the intensity, as determined with a phosphor imager, of the α_1-band to cyc-band and α_2-band to cyc-band in each domain to estimate the fraction of mRNA for the isoform. This normalization corrects for differences in the amount of material as well as exposure time in each domain. The cyc band in several of the lanes is visually weak but easily detected above background when measured with the phosphor imager. We should emphasize that to do this experiment, 50 lenses were dissected and their epithelial cells separated into anterior and equatorial pools to obtain a minimally detectable amount of material (less than 0.1 μg poly A^+ RNA per sample compared to a more typical sample of 5 μg). Nevertheless, the results identified the high DHO-affinity pumps as the α_2-isoform and the fraction of each isoform determined in Table 1 is consistent with the electrophysiological contributions of each isoform to total pump current. Based on these data and the DHO-blockade data, the α_2-isoform dominates in anterior epithelial cells but the α_1-isoform dominates in equatorial cells.

Whole Cell Patch Clamp

As described in Materials and Methods, surface cells that adhered to the lens capsule were separated into anterior and equatorial groups. These are the cells colored red in Fig. 1. If one visualizes the lens as a sphere with anterior pole (top of Fig. 1) at $\theta = 0°$, the equator at $\theta = 90°$ and the posterior pole at $\theta = 180°$, the anterior cells were from $\theta = 0$ to 45°, whereas equatorial surface cells were from 45 to about 100°, where the cells ceased to adhere to the capsule. When isolated, both the wide short anterior epithelial cells and the narrower longer equatorial epithelial cells become spheres with diameters of about 30 μm (*see* Fig. 1 of Cooper et al., 1989). Some of the

A

Rana p.	α1	SSPTWTALAR VAGLCNRAVF QAGQENTPIL KRDVAGDASE SALLKCIELC CGSVRDMREK NTKVAEIPFN CTNKY
Rana p.	α2	R.......SK I..... KV....T.IS ...T..... .....T..S .....K..D. .P..... R....
Rana p.	α3	.....V...R I.S..... K..ND.I.VL ....S ....KA..E. YK..... R....

B

Rana p.	α1	SSPTWTALAR VAGLCNRAVF QAGQENTPIL KRDVAGDASE SALLKCIELC CGSVRDMREK NTKVAEIPFN CTNKY
Human	α1	T.A..L..S. I..... .N...L.... .A..... ....KE...RY A.IV.....S .....
Rat	α1	T.A..F..S. I..... .N...L.... .A..... .....V.. ...ME....Y ..IV.....S .....
Chick	α1	..A..L..S. I..... .N...V.... .A..... ....KE...RY P..V.....S .....
Pig	α1	T.A..L..S. I..... .N...L.... .A..... ....KE...RY ..IV.....S .....
Dog	α1	..A..L..S. I..... .N...L.... .A..... ....KE..DRY A.IV.....S .....
Horse	α1	T.A..LS.S. I..... .N...I.... .A..... ....KE..DRY P.IV.....S .....
Sheep	α1	T.A..L..S. I..... .N.D.L.... .A..... .....V.. ...KE...RY A.IV.....S .....
Bufo m.	α1	..... I..... ....V..... ....K..... Q.....S .....

Rana p.	α2	RSPTWTALSK IAGLCNRAVF KVGQENTPIS KRDTAGDASE SALLKCTELS CGSVRKMRDK NPKVAEIPFN RTNKY
Human	α2	.....R ..... .A....ISV. ....I... .....R ..... S....
Rat	α2	.....R ..... .A....ISV. ....I... .....R ..... S....
Chick	α2	.....A...R ..... .P....IS.. ....IQ.. ....K..... ....T..... S....

Rana p.	α3	SSPTWVALAR IASLCNRAVF KAGNDNIPVL KRDVAGDASE SALLKCIELS CGSVKAMREK YKKVAEIPFN RTNKY
Human	α3	..H.....SH ..G..... .G.Q..... .... S....L...R N..... S....
Rat	α3	..H.....SH ..G..... .G.Q..... .... S....L...R N..... S....
Chick	α3	..A.....SH ..G..... .G.QE.V.I. .... S....V...R N..... S....
Pig	α3	T.A.....S. ..G..... Q.NQE.L.I. ..A..... .....C .....E...R .T.IV..... S....

C

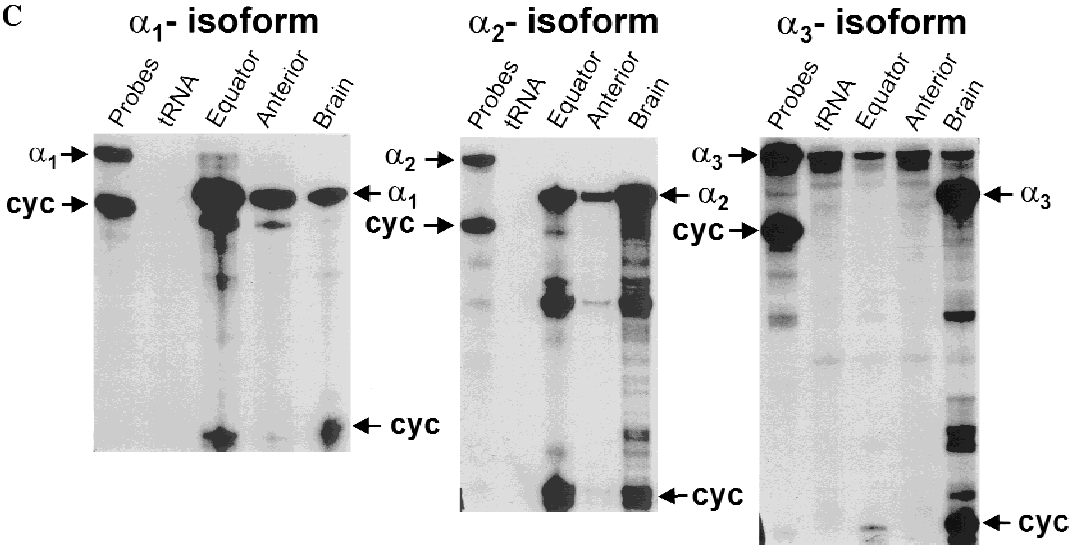

Fig. 3. The cloned fragments of α_1-, α_2- and α_3-isoforms of the Na/K pump and RNase protection assays for these isoforms. (*A*) The alignment of the amino acid sequences of the α_1-, α_2- and α_3-isoform fragments cloned from frog brain. (*B*) An inter species comparison of the amino acid sequences for each fragment cloned from frog brain. (*C*) RNase protection assays for the presence of α_1-, α_2-, and α_3-isoforms present in frog lens epithelial cells isolated from either the anterior or equatorial region of the lens.

isolated equatorial cells were more ellipsoidal in shape, with a major axis 2 to 3 times longer than the minor axis, indicating they had begun to differentiate into the elongated fiber cells. These are probably the long cells (shown in red in Fig. 1) that form additional layers of cells just at the equator. Because of this difference in shape (state of differentiation), we further classified equatorial cells as either epithelial or differentiating.

Table 1. Results of RNase assays for the α_1- and α_2-isoforms of the Na/K pumps in frog lens epithelium

	Anterior	Equator
α_1:cyc	13.7	33.4
% mRNA	23%	92%
α_2:cyc	44.7	2.8
% mRNA	77%	8%

These three classes of isolated cells were used for whole cell patch clamp studies. As described in Materials and Methods and shown in Fig. 2, Na/K pump current (I_P) was defined as the inward shift in current following application of the specific inhibitor of Na/K ATPase activity, dihydro-ouabain (DHO).

In studies of Na/K pump current in the larger more robust ventricular myocytes from guinea pig heart (Gao et al., 1995, 1997), the external Ca^{2+}-concentration appeared to not affect I_P in all conditions tested. As a control to determine if the Na/K pumps in frog lens epithelial cells are also insensitive to external Ca^{2+}, I_P was recorded from 20 equatorial cells in 2 mM $[Ca^{2+}]_o$ (0.76 ± 0.18 pA/pF) and compared to that recorded from 10 equatorial cells in 0 mM $[Ca^{2+}]_o$ (0.69 ± 0.13 pA/pF). To the accuracy of our data (mean ± SD), the lens Na/K pumps also appear to be insensitive to $[Ca^{2+}]_o$. Since the isolated epithelial cells are small and fragile and do not survive long in the presence of Ca^{2+}, all other pump experiments were carried out in Ca^{2+}-free Ringer.

DHO-Blockade of I_P in Anterior and Equatorial Cells

The first evidence for multiple isoforms of Na/K pumps in the lens came before the existence of different isoforms was known: Paterson et al. (1974) reported that the resting voltage of rabbit lenses had a biphasic response to varying concentrations of ouabain. The DHO-blockade studies shown in Fig. 4 suggest that more than one isoform is also present in the frog lens epithelium, and that different isoforms dominate in anterior *vs.* equatorial cells, just as suggested by the RNase protection assays. Without regard to the decomposition of the curves into contributions from the α_1-isoform (ΔI_{P1}) or α_2-isoform (ΔI_{P2}), the overall blockade curves were half-saturated at a DHO concentration of about 10^{-6} M anterior *vs.* 10^{-4} M equatorial. In most species, the α_1-isoform has about a 100-fold lower affinity for DHO than the α_2- or α_3-isoform (Sweadner, 1989) thus the curves immediately suggested the α_1-isoform is dominant at the equator whereas the α_2- or α_3-isoform dominates at the anterior pole. The RNase protection assays of the previous section confirmed this suggestion and identified the high DHO-affinity isoform as α_2.

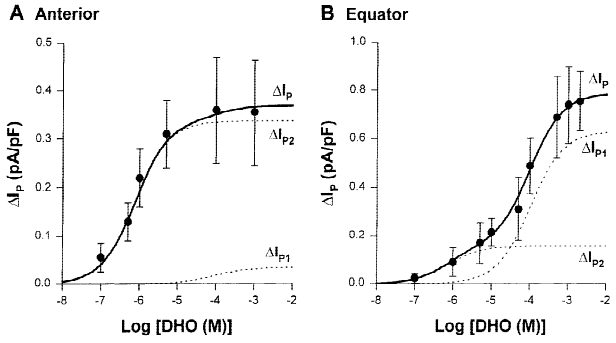

Fig. 4. DHO blockade of I_P. (*A*) DHO blockade of I_P in anterior epithelial cells. Data are mean ± SD from 5–9 cells for each point. The solid line is the best fit of Eq. 5 to the data, assuming 87% of the maximally inhibited current is generated by α_2-isoform. The dashed lines show the contributions of the α_1- and α_2-isoforms to the overall blockade curve. (*B*) DHO blockade of I_P in equatorial cells. Data are mean ± SD from 5–6 cells for each point. The theory curve are the same as described above, except in equatorial cells only 20% of the maximally inhibited current is due to the α_2-isoform. In either *A* or *B*, the dissociation constants are 100 μM for I_{P1} and 0.75 μM for I_{P2}.

Total pump current (I_P) in either anterior or equatorial cells is the sum of currents contributed by the α_1-isoform (I_{P1}) and the α_2-isoform (I_{P2}): $I_P = I_{P1} + I_{P2}$. At the constant $[Na^+]_i$, $[K^+]_o$ and pH_o, Eqs. 3 and 4 simplify to Eq. 5, which was used to fit data from either domain.

$$\Delta I_p = I_{max}\left[\frac{f_1[DHO]}{[DHO]+K_{D1}} + \frac{f_2[DHO]}{[DHO]+K_{D2}}\right] \quad (5)$$

The dashed lines show the contributions of ΔI_{P1}, the first term of the sum, and ΔI_{P2}, the second term. In the anterior cells we estimate I_{P2} contributes the major fraction of 91% of activity. In contrast, in equatorial cells we estimate I_{P2} contributes about 20% of total activity with I_{P1} contributing the major fraction of 80% of activity. This decomposition is shown by the dashed lines in Fig. 4. For either anterior or equatorial cells, the dissociation constants were K_{D2} = 0.75 μM and K_{D1} = 100 μM DHO. These fractional contributions and dissociation constants provide reasonable fits to the data in Fig. 4, however the standard deviations are sufficiently large that some variation in the fractions and dissociation constants would have provided equally good fits. We therefore chose the fractions of I_{P1} and I_{P2} based not only on the data in Fig. 4 but also on the RNase protection assays, data on $[K^+]_o$-activation (*see* Fig. 7), the effect of external pH on I_{P1}, and some reasonable assumptions. This process is described below.

At a $[K^+]_o$ of 8 mM, which was used for Fig. 4, I_{P1} is at 2/3 of saturation whereas I_{P2} is saturated. Based on data in Fig. 8 as well as results in Gao et al. (1995), at a pH_o of 7.35, which was used for Fig. 4, ATPase activity

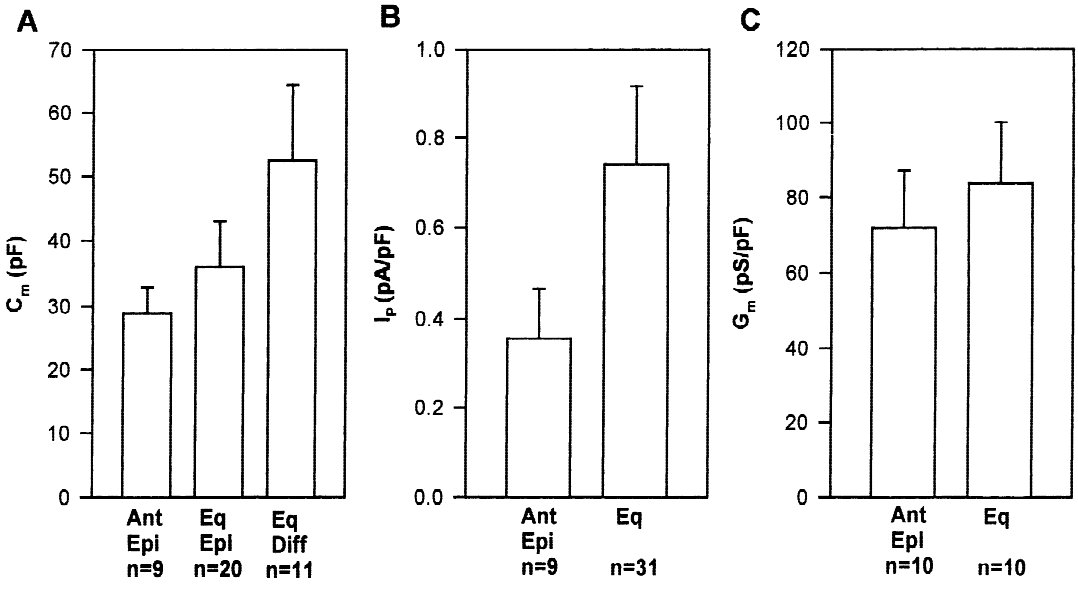

Fig. 5. A comparison of membrane capacitance, Na/K pump current and membrane conductance in anterior *vs.* equatorial lens cells. Bars indicate SD. (*A*) Total cell membrane capacitance (C_m) for anterior epithelial cells, equatorial epithelial cells and equatorial differentiating cells. These are the same cells in which Na/K pump current was measured. (*B*) Na/K pump current (I_P) normalized by C_m to control for variations in cell size. Although the equatorial differentiating cells generated a relatively large total current, when normalized by C_m, I_P was indistinguishable from that recorded in equatorial epithelial cells, hence all equatorial cell values of I_P are lumped together in panel *B*. (*C*) Membrane conductance (G_m) normalized by C_m to control for variation in cell size. These data were recorded in normal Ringer solution containing 2 mM $[Ca^{2+}]_o$ and no Ba^{2+} or Cd^{2+} that would block membrane ion channels.

of the α_1-isoform is at 1/2 its maximum whereas the α_2-isoform is unaffected by pH_o in this range. Overall, this suggests I_{P1} is about 1/3 of its maximal value whereas I_{P2} is essentially maximized. We made two assumptions: first, we assumed the maximum transport rate of the α_1- and α_2-isoforms is about the same on a per protein basis, and second, we assumed the mRNA in Table 1 is approximately proportional to the fractional amount of protein for each isoform. Thus the α_1:cyc ratio is divided by 3 and the contribution of each isoform to total current is recalculated to yield 9% I_{P1} in anterior cells *vs.* 80% I_{P1} in equatorial cells. This is essentially the same method as used in Gao et al. (1999) to estimate the fraction of α_1-protein *vs.* α_1-activity in guinea pig myocytes. In both instances, the conclusions fit the data from RNase assays and whole cell patch-clamp studies.

Na/K ATPase Activity and K^+-Conductance in Anterior *vs.* Equatorial Cells

As described in the section Whole Cell Patch Clamp, and as can be seen in Fig 5*A*, the equatorial differentiating cells were significantly larger than equatorial epithelial cells, however when transport properties per unit area of membrane (estimated by membrane capacitance, C_m) were determined, the equatorial epithelial and differentiating cells were statistically indistinguishable (I_P/C_m was 0.65 ± 0.17 pA/pF differentiating *vs.* 0.74 ± 0.17 pA/pF epithelial).

Figure 5*B* gives the Na/K pump current density in pA/pF, which is approximately $\mu A/cm^2$ of cell membrane. The average Na/K pump current density in equatorial cells is 0.71 pA/pF, which is about twice the value of 0.37 pA/pF for anterior cells. The differentiating equatorial cells are those nearest to $\theta = 90°$. These cells have an average C_m of 52 pF, which is nearly twice as large as the 29 pF per anterior cell. Thus, the total pump current in equatorial differentiating cells is about 3.4 times greater than that of anterior epithelial cells. Moreover, in the intact lens, the geometry of the equatorial cells, which are long and narrow, in contrast to that of anterior cells, which are short and wide, implies the Na/K pump current density per unit area of lens surface will be about 20 times greater at the equator (*see* Discussion).

Figure 5*C* shows G_m/C_m in equatorial and anterior cells. These experiments were done in the absence of extracellular Ba^{2+}, whereas in the presence of Ba^{2+} the conductance was 48 ± 17 pS/pF in either anterior or equatorial cells. Thus the Ba^{2+} sensitive conductance was 24 pS/pF for the anterior epithelial cells and 36 pS/pF for equatorial cells. These cells have a higher total conductance and more depolarized resting voltage than estimated in the intact frog lens (reviewed in Mathias et al., 1997). The average (anterior, posterior and equatorial) surface cell conductance is about 0.21 mS/cm^2, and the average surface capacitance about 5 $\mu F/cm^2$, hence the ratio estimated from intact lenses is 42 pS/pF. The

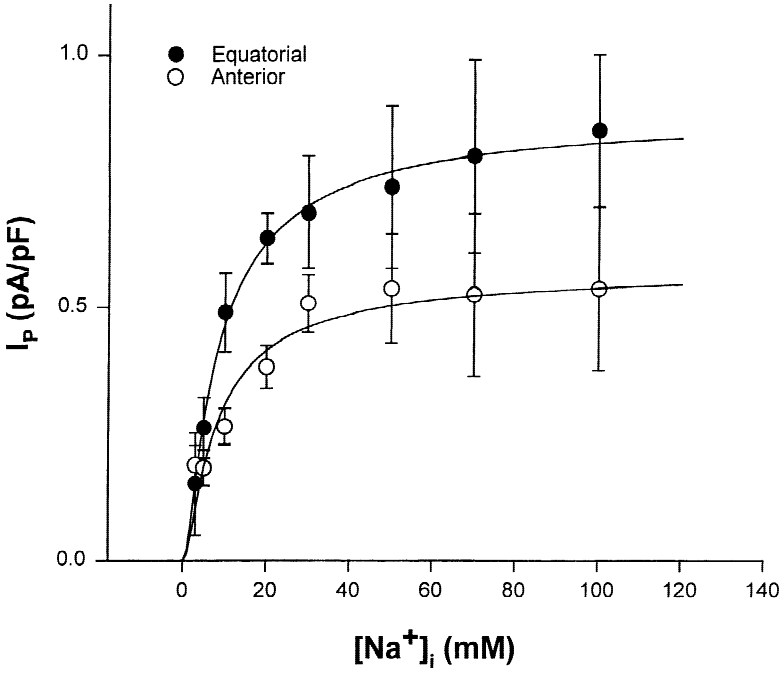

Fig. 6. The dependence of I_P on $[Na^+]_i$. The data are mean ± SD with each point representing 5 to 8 cells. The larger number of cells defined the critical points around the $K_{0.5}$. The theory curves were generated by Eq. 6 with a $K_{0.5}$ = 9 mM for either anterior or equatorial data.

isolation procedure may, therefore, have caused an increase in nonselective leak conductance. This limitation, and the large cell to cell variability make it difficult to know if there is any real difference in the anterior *vs.* equatorial cell membrane conductance.

The Dependence of Lens I_P on $[Na^+]_i$ and $[K^+]_o$

Energy dependent transport of Na^+ out of cells and K^+ into cells has been known to exist since the early 1950s. Post (1989) reviews the pioneering work linking the transport of these two ions together through the Na/K ATPase. The dependence of the Na/K pump on $[Na^+]_i$ and $[K^+]_o$ has been demonstrated in vesicles by measuring ATPase activity (Swann & Albers, 1975; Blostein, 1979; Drapeau & Blostein, 1980; Karlish & Pick, 1981; Karlish & Stein, 1985; Polvani & Blostein, 1989) and in intact cells by whole cell patch clamp measurement of I_P (Nakao & Gadsby, 1989; Gao et al., 1995). All of these studies suggest physiologically relevant variations in $[Na^+]_i$ or $[K^+]_o$ will alter I_P. The dependence of the Na/K pump on $[K^+]_i$ is not so well known, but Gao et al. (1995) found no detectable change in I_P when $[K^+]_i$ was reduced from 140 to 70 mM, suggesting this dependence occurs well above normal physiological $[K^+]_i$. Gadsby et al. (1993) showed that changes in $[Na^+]_o$ affect the voltage dependence of I_P, however a ±10 mM change in $[Na^+]_o$ causes only a $\mp$6–7% change in I_P. Thus, physiological variations in lens Na/K pump activity are most likely to be due to variations in $[Na^+]_i$ or $[K^+]_o$, and we have focused on these effects.

The Dependence of I_P on $[Na^+]_i$

The experiments in Fig. 6 were done by selecting a Na^+-concentration in the pipette, $[Na^+]_p$, performing a whole cell patch-clamp study using 1 mM DHO to measure I_P and a current step to measure C_m, then repeating this procedure with a new pipette and new cell. Since, I_{P2} dominates in anterior cells and I_{P1} in equatorial, this procedure should have detected any major difference in the $[Na^+]_i$-dependence of I_{P1} and I_{P2}. There was no difference in results from anterior *vs.* equatorial cells, however, so Eqs. 2 and 4 simplify Eq. 6, which was used to fit both data sets.

$$I_p = I_{max}\left(\frac{[Na^+]_i}{[Na^+]_i + K_{Na}}\right)^3 \qquad K_{Na} = \left(\sqrt[3]{2} - 1\right)K_{0.5} \tag{6}$$

The best fit values are, for anterior cells I_{max} = 0.58 pA/pF and $K_{0.5}$ = 9 mM, and for equatorial cells I_{max} = 0.89 pA/pF and $K_{0.5}$ = 9 mM. These values for half maximal activation by $[Na^+]_i$ are essentially the same as those for mammalian heart cells (Gadsby, Rakowski & DeWeer, 1993; Gao et al., 1995).

The data in Fig. 6 are graphed as a function of $[Na^+]_i$, assuming $[Na^+]_i \approx [Na^+]_p$. Mathias et al. (1990) and Gao et al. (1995) were concerned with differences between $[Na^+]_i$ and $[Na^+]_p$. Mathias et al. (1990) derived the relationship:

$$j_{Na} = \frac{D_{Na}\rho}{R_p}\left([Na^+]_p - [Na^+]_i\right) \tag{7}$$

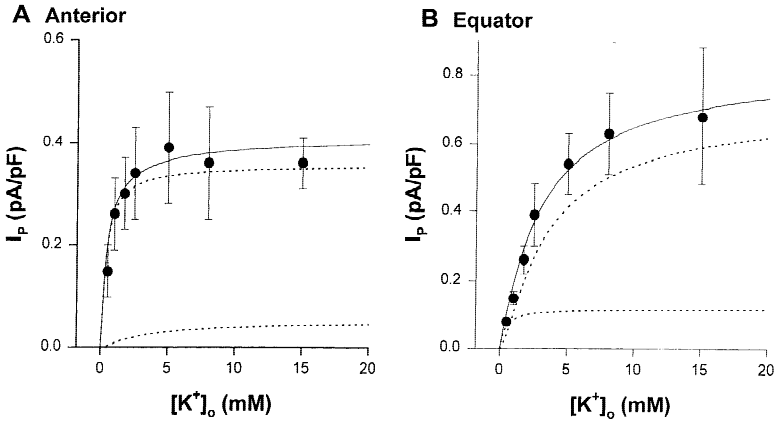

Fig. 7. The dependence of I_P on $[K^+]_o$. The data are mean ± SD, with each point representing 7–11 cells for the anterior data (*A*), and 5–15 cells for the equator (*B*). The solid lines represent the best fits of Eq. 8, with the dashed lines representing the contributions of I_{P1} and I_{P2} to $I_P = I_{P1} + I_{P2}$. In the anterior cells, 87% of the maximum ($[K^+]_o \rightarrow \infty$) current is from I_{P2}, whereas in equatorial cells, 86% of the maximum current is from I_{P1}. In either anterior or equatorial cells, the $K_{0.5}$ for I_{P1} was 3.9 mM $[K^+]_o$ and for I_{P2} was 0.4 mM $[K^+]_o$.

where j_{Na} (moles/s) is net Na^+-efflux from the cell, D_{Na} (cm^2/sec) is the diffusion constant for Na^+, R_p (Ω) is the pipette resistance and ρ (Ω-cm) is the resistivity of pipette solution. Gao et al. (1995) used this relationship to correct the $[Na^+]_i$-dependence of I_P for differences between $[Na^+]_i$ and $[Na^+]_p$. This correction shifted their value of $K_{0.5}$ from 14 mM $[Na^+]_p$ to 9 mM $[Na^+]_i$, a shift of 5 mM. However, cardiac myocytes are much bigger than lens epithelial cells and consequently the value of j_{Na} is much larger in the myocytes. Using the same procedure described in Gao et al. (1995), the $K_{0.5}$ for the curves in Fig. 6 would be shifted by less than 1 mM. We did not make this correction.

The Dependence of I_P on $[K^+]_o$

The activation of total pump current, $I_P = I_{P1} + I_{P2}$, in anterior cells (Fig. 7*A*) was half-saturated at $[K^+]_o$ of 0.6 mM, whereas that for equatorial cells (Fig. 7*B*) was half-saturated at a $[K^+]_o$ of 3 mM, suggesting I_{P1} and I_{P2} had very different sensitivities to $[K^+]_o$. At the constant $[Na^+]_i$, $[K^+]_o$ and pH_o, Eqs. 2 and 4 simplify to Eq. 8, which was used to fit data from both anterior and equatorial cells.

$$I_p = I_{max}\left[F_1\left(\frac{[K^+]_o}{[K^+]_o + K_{K1}}\right)^2 + F_2\left(\frac{[K^+]_o}{[K^+]_o + K_{K2}}\right)^2\right] \qquad (8)$$

$$K_K = \left(\sqrt{2} - 1\right)K_{0.5}$$

The fractions F_1 of I_{P1} and F_2 of I_{P2} were estimated as described for the DHO-binding curves in Fig. 4. However, for DHO-binding, $[K^+]_o$ was 8 mM so I_{P1} was at 2/3 saturation whereas in Fig. 7, F_1 and F_2 refer to the fractions at saturation, when $[K^+]_o \rightarrow \infty$. We therefore divided the α_1:cyc ratio by 2 to account for pH_o effects, then calculated the fraction of I_{P1} at $[K^+]_o \rightarrow \infty$ would be 13% in anterior cells and 86% in equatorial cells. The best fit values of $K_{0.5}$ were 3.9 mM $[K^+]_o$ for I_{P1} and 0.4 mM $[K^+]_o$ for I_{P2}, almost identical to the values for the mammalian versions of I_{P1} and I_{P2} (Gao et al., 1995).

INHIBITION OF I_{P1} BY EXTERNAL pH

There have been a number of reports that pH modifies Na/K ATPase activity (Skou & Esmann, 1980, 1992; Skou, 1982, 1984). In mammalian cardiac myocytes, physiological variations in external pH affects transport by the α_1-isoform but not the α_2-isoform of the Na/K pump (Gao et al., 1995). In those cells, an increase in pH_o increased I_{P1} and a decrease inhibited I_{P1}. This dependence on pH_o suggested transport was inhibited by the binding of H^+ to an external site with a pK of about 7.7. The isolated lens epithelial cells were difficult to seal and ran down rapidly at other than normal pH_o of 7.35. Nevertheless, we were able to demonstrate in Fig. 8 that the amphibian isoforms are similar to their mammalian counterparts with regard to pH_o effects.

Figure 8*A* shows a drop in pH_o from 7.35 to 6.8 has no significant effect on anterior cells, where the α_2-isoform generated 91% of I_P. Assuming the drop in pH_o affects only I_{P1}, it should reduce anterior I_P by 3 to 4%. Since the SD is on the order of ±25%, such small effects cannot be detected by the methods used here. In contrast, in the equatorial cells, where the α_1-isoform generated 80% of I_P, Fig. 8*B* shows a drop in pH_o from 7.35 to 6.8 caused a significant inhibition of I_P. The reduction in I_P suggests about a 40% inhibition of I_{P1}. If this response is similar to that found in mammalian cells, with regard to inhibition being due to H^+ binding to an external site on the α_1-isoform, then the frog lens α_1-isoform site has a pK of about 7.3. If so, then at normal pH_o, the α_1-isoform is running at about 50% of the rate of transport that could be achieved in the absence of H^+-binding. We clearly lack the data at alkaline pH_o to support this hypothesis, however it is consistent with other results in this paper. For example, RNase protection assays sug-

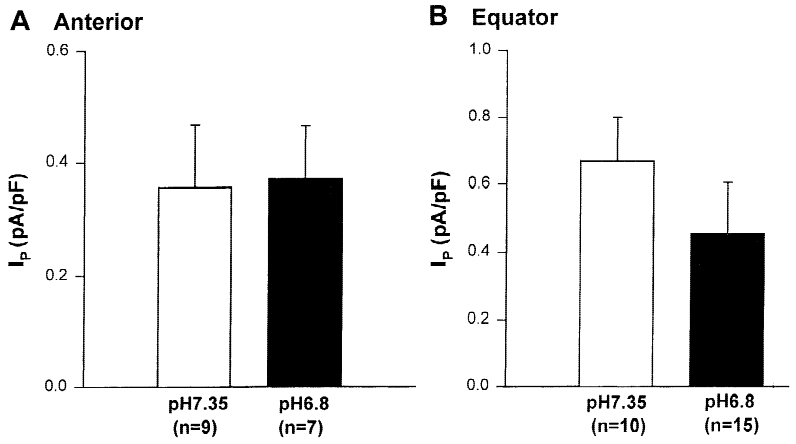

Fig. 8. The effect of external pH on I_P. (*A*) In the anterior cells, where the α_1-isoform generates just 9% of I_P under the conditions of the experiments, a drop in pH_o from 7.35 to 6.8 has no detectable effect. (*B*) In equatorial cells, where the α_1-isoform generates an estimated 80% of I_P, a drop in pH_o from 7.35 to 6.8 causes a 32% inhibition of I_P. Panels *A* and *B* together suggest the change in pH_o from 7.35 to 6.8 does not affect I_{P2} but inhibits I_{P1} by about 40%.

gest the anterior α_1-isoform is 23% of total protein but our patch clamp results indicate it is just 13% of I_P (at saturating $[K^+]_o$). Similarly, our data suggest the equatorial α_1-isoform is 92% of total pump protein but 86% of I_P. Both of these discrepancies are consistent with I_{P1} running at about 50% of its maximum rate, but I_{P2} running at maximum rate.

Discussion

The results presented here are the first direct measurements of Na/K pump current in the lens, and as such they have provided significant new information. In frog lens, the α_1-isoform of the Na/K pump is the dominant presence in equatorial cells whereas the α_2-isoform is dominant at the anterior pole. Both isoforms are half maximally activated at an $[Na^+]_i$ of 9 mM, a value very close to normal physiological $[Na^+]_i$. Hence both isoforms are poised to respond maximally to any change in $[Na^+]_i$. A normal physiological $[K^+]_o$ of around 4 mM is saturating for the α_2-isoform, which is half maximally activated at 0.4 mM $[K^+]_o$, whereas it is half-saturating for the α_1-isoform. Thus, the α_1-isoform is poised to respond maximally to changes in $[K^+]_o$, but the α_2-isoform works independently of normal physiological variations in $[K^+]_o$. Furthermore, a drop in external pH inhibits ATPase activity by the α_1-isoform, but has no effect on the α_2-isoform. Lastly, the Na/K pump current density in equatorial cells is about twice that in anterior cells, and the larger current density persists as the equatorial cells begin to differentiate.

Implications for the Intact Lens

As was described in the Introduction, the hypothesis that the circulating current shown in Fig. 1 is carried by Na^+ is consistent with several properties of the lens. However, this hypothesis lacked a specific mechanism for transporting Na^+ out of the equatorial cells. The geometry of lens epithelial and differentiating cells (Kuszak, Bertram & Rae, 1986) in connection with the results described here suggest the Na/K pump current per area of lens surface is concentrated at the equator.

Although Fig. 1 is not drawn to scale, it illustrates the relatively wide and short anterior cells in contrast to the narrow and long equatorial cells. Clearly, a polar cell occupies a much greater area of lens surface than an equatorial cell. This difference in geometry has a very large effect on the Na/K pump current density per area of lens surface. If a typical anterior cell is a cuboid, 32 μM wide by 6 μM high, it will have a membrane area of 28×10^{-6} cm^2, so a membrane capacitance of 1 $\mu F/cm^2$ would yield the 28 pF input capacitance reported in Fig. 5. These dimensions are typical of the anterior epithelial cells shown in Kuszak et al. (1986, Fig. 1*a*). Moreover, such a cell will occupy about 10×10^{-6} cm^2 of lens surface area. As one looks closer to the equator, the epithelial cells are narrower but longer, with typical dimensions of about 20 μm in width and 30 μm in height (Kuszak et al., 1986, Fig. 1*d*). A cuboidal cell of these dimensions will have a total membrane area of about 32×10^{-6} cm^2, and an input capacitance of about 32 pF, similar to the value in Fig. 5. This cell, however, occupies just 4×10^{-6} cm^2 of lens surface area. Lastly, at the equator, the differentiating cells get very long and actually lay beneath other equatorial epithelial cells (*see* the long equatorial cells colored in red in Fig. 1). These, we believe, are the equatorial cells we refer to as "differentiating". There are actually many more such cells than shown in Fig. 1, and the reader should look at Kuszak et al. (1986; Fig. 2*a*) for a better perspective. Such a cell of width 12 μm and length 100 μm will have a membrane area of 51×10^{-6} cm^2 and an input capacitance of 51 pF (similar to Fig. 5), but it occupies only 1.44×10^{-6} cm^2 of lens surface area. One way to think about this effect of geometry is that several cell layers contribute to the equatorial pump current in an intact lens (*see* Fig. 1).

A more quantitative estimate can be obtained by taking the average pump current per cell in normal physiological conditions, then divide by the area of lens surface occupied by that cell to obtain an estimate of the pump current density per area of lens surface.

The values of I_P reported in Fig. 5*B* were obtained in 50 mM $[Na^+]_i$. At normal physiological conditions, the value of $[Na^+]_i$ is around 9 mM, which will reduce anterior I_P to about 50% of the value in Fig. 5*B.* Given the average capacitance from Fig. 5*A* is 28 pF, the normal physiological pump current per cell is 5 pA. To estimate the pump current density per area of lens surface, we divide the 5 pA by 10×10^{-6} cm^2, which gives a typical pump current density at the anterior pole of about 0.5 $\mu A/cm^2$. Note that neither our data nor this calculation implies anything about the apical *vs.* basolateral localization of pump protein. The calculation simply associates the measured total cellular pump current with the appropriate area of lens surface. Taking into account the effect of high $[K^+]_o$ and $[Na^+]_i$ on the equatorial pump current data in Fig. 5*B*, in physiological conditions the pump current should be about 30% of the value in Fig. 5*B.* The pump current per differentiating cell is therefore around 11.5 pA, which, when divided by 1.44×10^{-6} cm^2, gives a pump current density per area of equatorial surface of 10 $\mu A/cm^2$, a value 20 times larger than that at the anterior pole.

The above estimated values can be compared to measurements from intact lenses. Given the stoichiometry of the Na/K pump is $3Na^+/2K^+$ (Post, 1989), for a pump current density of 10 $\mu A/cm^2$, the Na^+-current actively transported out of the equatorial cells will be 30 $\mu A/cm^2$. This value is very close to the average peak outward equatorial current of 26 $\mu A/cm^2$ measured with the vibrating probe in frog lens (Parmelee, 1986). However, there is also an influx of K^+ generated by the Na/K pumps, but this influx is in large part balanced by the passive electrodiffusion of K^+ out of the equatorial cells, which have a significant K^+-conductance. For simplicity, assume the active uptake and passive efflux of K^+ balance exactly, so all of the measured equatorial outward current is carried by Na^+. If ouabain is applied externally to a lens, it will block all Na/K pump current, however the equatorial current will be reduced by just 1/3 or 33%. With active transport of both Na^+ and K^+ blocked, outward current becomes entirely electrodiffusion of K^+. Thus, Na^+ will accumulate and K^+ will deplete and with time the circulating current will approach zero. In frog lens, application of ouabain causes an initial decrease in the circulating current of approximately 30% (Parmelee, 1986), very similar to the 33% predicted by the above idealized calculation, then it slowly declines toward zero.

In the vibrating probe experiments described above, different surfaces of the lens were not isolated, hence ouabain accesses all surfaces. Moreover, ouabain affects the entire current loop (*see* Fig. 1), reducing inward current at the poles the same as outward current at the equator. Those studies, therefore, did not provide information on the localization of Na/K pumps. In an abstract, Zamudio, Candia & Alvasey (1998), described the effect of ouabain on the isolated anterior, posterior and equatorial surfaces of the rabbit lens. They reported that ouabain only had a measurable effect when applied equatorially, where it blocked a current of about 10 $\mu A/cm^2$. Again, this value is consistent with our rough calculations of the pump current density at the frog lens equator. The lack of measurable changes in current when ouabain was applied to the anterior polar region is also consistent with our estimated pump current density of 0.5 $\mu A/cm^2$, which is in the noise level of whole lens currents.

In summary, the data reported here fit well with intact lens data, which were obtained by very different methods. The above calculations are obviously idealized and the assumed values of cell size are crude estimates from a few pictures of freeze fractured lenses. Nevertheless, all of the existing data are consistent with the hypothesis that the circulating current is carried primarily by Na^+, and the outward current at the equator is generated by the active extrusion of Na^+ via Na/K pumps, which are concentrated at the lens equator.

Roles of Different Isoforms

An interesting and open question is the physiological purpose of the isoform switch in going from anterior to equatorial cells. The data reported here show the two isoforms expressed in frog lens respond differently to the external ionic environment. At the equator, the small intercellular spaces between surface cells extend deeper into the lens than at the anterior pole (*see* Fig. 1), so there is a possibility of more extracellular accumulation/depletion of ions such as K^+ or H^+. However, without knowing more about the specific localization of Na/K pump protein in the membranes of equatorial cells, it is not possible to estimate how the ionic environment might affect the Na/K pumps, or how the Na/K pumps might regulate extracellular K^+-concentration. In man, acidosis is usually accompanied by an increase in extracellular K^+-concentration, so these two changes should have offsetting effects on transport by the α_1-isoform of the Na/K pumps. Since the same effects were found for the mammalian version of the α_1-isoform, this could be a general protective mechanism to maintain Na^+ homeostasis during acidosis. We also reported in mammalian cells that the α_1- and α_2-isoforms of the Na/K pump are coupled to norepinephrine levels through different receptors and different signal transduction cascades (reviewed in Mathias et al., 2000). Thus, another intriguing possibility is that the isoform switch in the lens is for the purpose

of regulation of the circulating current. For example, to upregulate the current, it would be ideal to increase α_1-mediated outward equatorial pump current without increasing the α_2-mediated outward anterior pump current, which is opposite in direction to the circulation. Hence, our next goal is to determine how hormones and neurotransmitters might differentially affect the isoforms of the lens Na/K pumps.

This work was supported by National Institutes of Health grants EY06391 and HL54031. We thank Dr. Ira Cohen for a careful and critical reading of a preliminary version.

References

Baldo, G.J., Mathias, R.T. 1992. Spatial variation in membrane properties in the intact rat lens. *Biophys. J.* **68:**518–529

Blostein, R. 1979. Side-specific effects of sodium on (Na,K)-ATPase. Studies with inside-out red cell membrane vesicles. *J. Biol. Chem.* **254:**6673–6677

Cooper, K., Rae, J.L., Gates, P. 1989. Membrane and junctional properties of dissociated frog lens epithelial cells. *J. Membrane Biol.* **111:**215–227

Drapeau, P., Blostein, R. 1980. Interactions of K^+ with (Na,K)-ATPase orientation of K^+-phosphatase sites studied with inside-out red cell membrane vesicles. *J. Biol. Chem.* **255:**7827–7834

Gadsby, D.C., Rakowski, R.F., De Weer, P. 1993. Extracellular access to the Na,K pump: pathway similar to ion channel. *Science* **260:** 100–103

Gao, J., Wymore, R., Wymore, R.T., Wang, Y., McKinnon, D., Dixon, J.E., Mathias, R.T., Cohen, I.S., Baldo, G.J. 1999. Isoform-specific regulation of the sodium pump by α- and β-adrenergic agonists in the guinea-pig ventricle. *J. Physiol.* **516:**377–383

Gao, J., Mathias, R.T., Cohen, I.S., Baldo, G.J. 1995. Two functionally different Na/K pumps in cardiac ventricular myocytes. *J. Gen. Physiol.* **106:**995–1030

Garner, M.H. 1994. Na,K-ATPases of the lens epithelium and fiber cell: formation of catalytic cycle intermediates and Na^+:K^+ exchange. *Exp. Eye Res.* **58:**705–718

Garner, M.H., Horwitz, J. 1994. Catalytic subunit isoforms of mammalian lens Na,K-ATPase. *Curr. Eye Res.* **13:**65–77

Garner, M.H., Kong, Y. 1999. Lens epithelium and fiber Na,K-ATPases: distribution and localization by immunocytochemistry. *Invest. Ophthalmol. Vis. Sci.* **40:**2291–2298

Karlish, S.J., Pick, U. 1981. Sidedness of the effects of sodium and potassium ions on the conformational state of the sodium-potassium pump. *J. Physiol.* **312:**505–529

Karlish, S.J., Stein, W.D. 1985. Cation activation of the pig kidney sodium pump: transmembrane allosteric effects of sodium. *J. Physiol.* **359:**119–149

Kreig, P.A., Melton, D.A. 1987. In vitro RNA synthesis with SP6 RNA polymerase. *Meth. Enzymol.* **155:**397–415

Kuszak, J.R., Bertram, B.A., Rae, J.L. 1986. The ordered structure of the crystalline lens. *In:* Development of Order in the Visual System. S.R. Hilfer and J.B. Sheffield, editors. pp. 35–60. Springer-Verlag, New York

Mathias, R.T., Rae, J.L. 1985. Transport properties of the lens. *Am. J. Physiol.* C181–C198

Mathias, R.T. 1985. Steady-state voltages in the frog lens. *Biophys. J.* **4:**421–430

Mathias, R.T., Cohen, I.S., Oliva, C. 1990. Limitations of the whole cell patch clamp technique in the control of intracellular concentrations. *Biophys. J.* **58:**759–770

Mathias, R.T., Rae, J.L., Baldo, G.J. 1997. Physiological properties of the normal lens. *Physiol. Rev.* **77:**21–50

Mathias, R.T., Cohen, I.S., Gao, J., Wang, Y. 2000. Isoform specific regulation of the Na/K pump in heart. *NIPS (in press).*

Moseley, A.E., Dean, W.L., Delamere, N.A. 1996. Isoforms of Na, K-ATPase in rat lens epithelium and fiber cells. *Invest. Opthal. Visual Sci.* **37:**1502–1508

Nakao, M., Gadsby, D.C. 1989. [Na] and [K] dependence of the Na/K pump current-voltage relationship in guinea pig ventricular myocytes. *J. Gen. Physiol.* **94:**539–565

Parmelee, J.T. 1986. Measurement of steady currents around the frog lens. *Exp. Eye Res.* **42:**433–441

Paterson, C.A., Neville, M.C., Jenkins, R.M., Nordstrom, D.K. 1974. Intracellular potassium activity in frog lens determined using ion specific liquid ion-exchanger filled microelectrodes. *Exp. Eye Res.* **19:**43–48

Polvani, C., Blostein, R. 1989. Effects of cytoplasmic sodium concentration on the electrogenicity of the sodium pump. *J. Biol. Chem.* **264:**15182–15185

Post, R.L. 1989. Seeds of sodium, potassium ATPase. *Annu. Rev. Physiol.* **51:**1–15

Robinson, K.R., Patterson, J.W. 1983. Localization of steady currents in the lens. *Curr. Eye Res.* **2:**843–847

Skou, J.C. 1982. The effect of pH, of ATP and of modification with pyridoxal 5-phosphate on the conformational transition between the Na^+-form and the K^+-form of the (Na^+ + K^+)-ATPase. *Biochim. Biophys. Acta* **688:**369–380

Skou, J.C. 1984. Effect on the equilibrium between the Na^+-form and the K^+-form of the (Na^+ + K^+)-ATPase of modification of the enzyme with pyridoxal 5-phosphate. *Biochim. Biophys. Acta* **789:**44–50

Skou, J.C., Esmann, M. 1980. Effects of ATP and protons on the Na:K selectivity of the (Na^+ + K^+)-ATPase studied by ligand effects on intrinsic and extrinsic fluorescence. *Biochim. Biophys. Acta* **601:**386–402

Skou, J.C., Esmann, M. 1992. The Na,K-ATPase. *J. Bioenerg. Biomembr.* **24:**249–261

Swann, A.C., Albers, W. 1975. Sodium + potassium-activated ATPase of mammalian brain. Regulation of phosphatase activity. *Biochim. Biophys. Acta* **382:**437–456

Sweadner, K.J. 1989. Isozymes of the Na/K ATPase. *Biochim et Biophys. Acta* **999:**185–200

Tao, Q.F., Hollenberg, N.K., Graves, S.W. 1999. Sodium pump inhibition and regional expression of sodium pump alpha-isoforms in lens. *Hypertension* **34:**1168–1174

Varadaraj, K., Kushmerick, C., Baldo, G.J., Bassnett, S., Shiels, A., Mathias, R.T. 1999. The role of MIP in lens fiber cell membrane transport. *J. Membrane Biol.* **170:**191–203

Wymore, R.S., Gintant, G.A., Wymore, T.R., Dixon, J.E., McKinnon, D., Cohen, I.S. 1997. Tissue and species distribution of mRNA for the I_{ks}-like channel. *Cir. Res.* **80:**261–268

Zamudio, A., Candia, O.A., Alvasey, L. 1998. Distribution of ionic conductances around the surface of the rabbit lens. *Invest. Opthalmol. Vis. Sci.* **39:**S790